GNSS Attitude Determination for Remote Sensing: On the Bounding of the Multivariate Ambiguity Objective Function

Nandakumaran Nadarajah, Peter J.G. Teunissen, and Gabriele Giorgi

Abstract

Global Navigation Satellite Systems (GNSS)-based attitude determination is a viable alternative for traditional methods such as gyroscopes. Precise attitude determination using multiple GNSS antennas mounted on a remote sensing platform relies on successful resolution of the integer carrier phase ambiguities. The Multivariate Constrained (MC-) LAMBDA method has been developed for the multivariate quadratically constrained GNSS attitude model that incorporates the known antenna geometry. In this contribution, it is demonstrated that the currently used easy-to-compute MC-LAMBDA bounding functions are relatively loose bounds that may result in too large integer search times. To mitigate this problem, we develop alternative bounding functions and compare their performance using simulated as well as real data. As a result we are able to identify tighter bounding functions that improve the search algorithms for instantaneous GNSS attitude determination.

Keywords

GNSS • Attitude determination • Constrained Integer Least-Squares • MC-LAMBDA • Carrier Phase Ambiguity Resolution

1 Introduction

Precise attitude determination is a prerequisite for remote sensing applications. For instance, estimating pointing directions for remote sensors such as radars and laser scanners requires the knowledge of platform orientation. Multiple GNSS receivers/antennas rigidly mounted on the platform can be used to determine platform orientation (see, for example, Cohen 1992; Lu 1995; Crassidis and Markley 1997; Li et al. 2004; Lin et al. 2004; Madsen and Lightsey 2004; Psiaki 2006). GNSS-based attitude determination system offers several advantages including that it is driftless and requires less maintenance.

Precise attitude determination using multiple GNSS antennas mounted on a platform relies on successful resolution of the integer carrier phase ambiguities. The Least squares AMBiguity Decorrelation Adjustment (LAMBDA) method is currently the standard method for solving unconstrained GNSS ambiguity resolution problems. For unconstrained and linearly constrained GNSS models, the method is known to be optimal in the sense that it provides integer ambiguity solutions with the highest possible success-rate.

In this contribution we focus on the problem of fixing the correct integer ambiguities for data collected on a frame of antennas firmly mounted on a rigid platform: the relative

N. Nadarajah (✉)
Department of Spatial Sciences, GNSS Research Centre, Curtin University, GPO Box U1987, Perth, WA 6845, Australia
e-mail: N.Nadarajah@Curtin.edu.au

P.J.G. Teunissen
Department of Spatial Sciences, GNSS Research Centre, Curtin University, GPO Box U1987, Perth, WA 6845, Australia

Delft Institute of Earth Observation and Space Systems (DEOS), Delft University of Technology, PO Box 5058, 2600 GB Delft, The Netherlands

G. Giorgi
Institute for Communications and Navigation, Technische Universität München, Munich, Germany

C. Rizos and P. Willis (eds.), *Earth on the Edge: Science for a Sustainable Planet*, International Association of Geodesy Symposia 139, DOI 10.1007/978-3-642-37222-3_67,

positions between the antennas are assumed to be known and constant, which result in a set of nonlinear constraints posed on the baseline vectors and can be exploited to strengthen the underlying observation model (attitude model). To exploit these constraints, we make use of the Multivariate Constrained (MC-) LAMBDA method (Teunissen 2007). Due to these nonlinear constraints, the search space of integer ambiguities is no longer ellipsoidal. This requires, so as to guarantee computational efficiency, special methods for the evaluation of the nonlinear multivariate ambiguity objective function.

In this contribution, we illustrate the principles of the MC-LAMBDA method and develop various easy-to-compute lower and upper bounding functions for the MC-LAMBDA objective function. We analyze their effect on MC-LAMBDA's search technique, namely, the search and shrink method. It is demonstrated that the currently used bounding functions are relatively loose bounds that may result in too large integer search times. To mitigate this problem, we develop alternative bounding functions and compare their performance using simulated as well as real data. As a result we are able to identify tighter bounding functions that improve the search algorithms for instantaneous GNSS attitude determination.

2 The GNSS-Based Attitude Determination

Let us consider a set of $r + 1$ antennas simultaneously tracking the same $s+1$ GNSS satellites on a single frequency. The set of linearized Double Difference (DD) GNSS phase and code observations obtained on the r baselines can be cast into a *multivariate* Gauss–Markov model as follows:

$$\mathrm{E}(Y) = AZ + GB \qquad Z \in \mathbb{Z}^{s\times r}, B \in \mathbb{R}^{3\times r} \quad (1)$$

$$\mathrm{D}(\mathrm{vec}(Y)) = Q_{YY} = P \otimes Q_{yy} \quad (2)$$

where $\mathrm{E}(\cdot)$ and $\mathrm{D}(\cdot)$ denote the expectation and dispersion operator, $\otimes$ denotes the Kronecker product, $Z = [z_1, \ldots, z_r]$ is the $s \times r$ matrix of r unknown DD integer ambiguity vectors z_i, $B = [b_1, \ldots, b_r]$ the $3 \times r$ matrix of r unknown baseline vectors b_i, G is the $2s \times 3$ geometry matrix that contains the unit line-of-sight vectors, A is the $2s \times s$ matrix that links the DD data to the integer ambiguities, and P and Q_{yy} are known matrices of order $r \times r$ and $2s \times 2s$, respectively. Here, $\mathrm{vec}(\cdot)$ denotes the vec-operator, which transforms a matrix into a vector by stacking the columns of the matrix one underneath the other. Matrix P takes care of the correlation that follows from the fact that the r baselines have one antenna in common and matrix Q_{yy} takes care of the precision of the phase and code data.

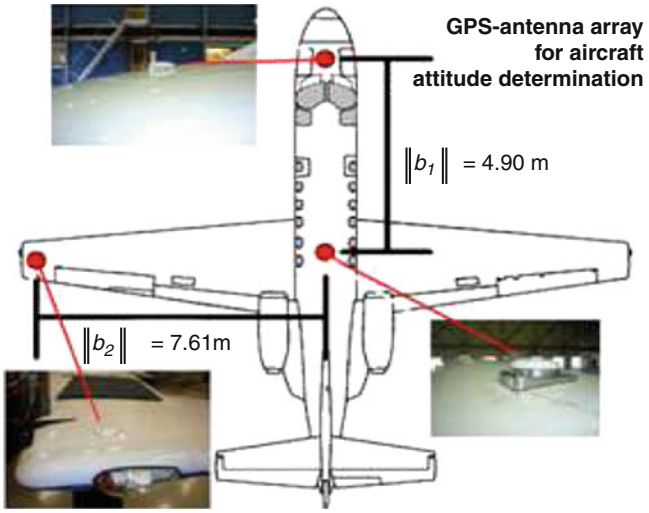

Fig. 1 Antenna geometry of the aircraft experiment

Model (1) can be strengthened by making use of the a priori known body-frame antenna geometry. This allows us to reparametrize B as

$$B = RB_0 \quad (3)$$

with the unknown $3 \times q$ orthogonal matrix R ($R^T R = I_q$) and the known $q \times r$ matrix B_0 describing the known geometry of the antenna configuration in the body-frame (q is the dimension of the span of the r baselines). For example, the local body-frame coordinate matrix B_0 is given by (31) for the three GNSS antennas shown in Fig. 1 and B refers to the corresponding coordinates in local East-North-Up (ENU) system, and then R represents the rotation from the local body-frame system to the local ENU system. Introducing this relation into model (1), gives the GNSS attitude model

$$\mathrm{E}(Y) = AZ + GRB_0 \qquad Z \in \mathbb{Z}^{s\times r}, R \in \mathbb{O}^{3\times q} \quad (4)$$

$$\mathrm{D}(\mathrm{vec}(Y)) = Q_{YY} = P \otimes Q_{yy} \quad (5)$$

Our goal is to solve the above system in a least-squares sense, while taking the integer constraints on Z and the orthonormality constraints on R into account. Hence, the minimization problem that will be solved reads

$$\min_{Z\in\mathbb{Z}^{s\times r}, R\in\mathbb{O}^{3\times q}} \|\mathrm{vec}\,(Y - AZ - GRB_0)\|^2_{Q_{YY}} \quad (6)$$

with $||\cdot||^2_Q = (\cdot)^T Q^{-1}(\cdot)$. The above problem does not admit a closed-form solution. In the following, we describe a three-step procedure for solving (6).

Float solutions: Using an orthogonal decomposition of the objective function, problem (6) can be written as:

$$\min_{Z\in\mathbb{Z}^{s\times r},R\in\mathbb{O}^{3\times q}} \|\mathrm{vec}\,(Y-AZ-GRB_0)\|^2_{Q_{YY}}$$
$$= \left\|\mathrm{vec}\left(\hat{E}\right)\right\|^2_{Q_{YY}} + \min_{Z\in\mathbb{Z}^{s\times r}}\left(\left\|\mathrm{vec}\left(\hat{Z}-Z\right)\right\|^2_{Q_{\hat{Z}\hat{Z}}}\right.$$
$$\left. + \min_{R\in\mathbb{O}^{3\times q}}\left\|\mathrm{vec}\left(\hat{R}(Z)-R\right)\right\|^2_{Q_{\hat{R}(Z)\hat{R}(Z)}}\right) \quad (7)$$

with $\hat{E}$ the matrix of least-squares residuals. For this decomposition we need $\hat{Z}$, $\hat{R}(Z)$ and their inverse-variance matrices. The so-called float solutions $\hat{Z}$ and $\hat{R}$, and their variance-covariance matrices, follow from

$$N\cdot\begin{bmatrix}\mathrm{vec}(\hat{Z})\\ \mathrm{vec}(\hat{R})\end{bmatrix} = \begin{bmatrix}I_s\otimes A^T\\ B_0\otimes G^T\end{bmatrix} Q_{YY}^{-1}\mathrm{vec}(Y) \quad (8)$$

$$N = \begin{bmatrix}I_s\otimes A^T\\ B_0\otimes G^T\end{bmatrix} Q_{YY}^{-1}\begin{bmatrix}I_s\otimes A & B_0^T\otimes G\end{bmatrix} \quad (9)$$

and

$$\begin{bmatrix}Q_{\hat{Z}\hat{Z}} & Q_{\hat{Z}\hat{R}}\\ Q_{\hat{R}\hat{Z}} & Q_{\hat{R}\hat{R}}\end{bmatrix} = N^{-1} \quad (10)$$

while the Z-constrained solution of R and its variance-covariance matrix are given as

$$\mathrm{vec}\left(\hat{R}(Z)\right) = \mathrm{vec}(\hat{R}) - Q_{\hat{R}\hat{Z}}Q_{\hat{Z}\hat{Z}}^{-1}\mathrm{vec}\left(\hat{Z}-Z\right) \quad (11)$$

$$Q_{\hat{R}(Z)\hat{R}(Z)} = Q_{\hat{R}\hat{R}} - Q_{\hat{R}\hat{Z}}Q_{\hat{Z}\hat{Z}}^{-1}Q_{\hat{Z}\hat{R}} \quad (12)$$

Ambiguity resolution: The multivariate constrained minimization problem in (7) is equivalent to minimizing the cost function $C(Z)$:

$$\check{Z} = \arg\min_{Z\in\mathbb{Z}^{s\times r}} C(Z) \quad (13)$$

where

$$C(Z) = \left\|\mathrm{vec}(\hat{Z}-Z)\right\|^2_{Q_{\hat{Z}\hat{Z}}} + \left\|\mathrm{vec}\left(\hat{R}(Z)-\check{R}(Z)\right)\right\|^2_{Q_{\hat{R}(Z)\hat{R}(Z)}} \quad (14)$$

with

$$\check{R}(Z) = \arg\min_{R\in\mathbb{O}^{3\times q}}\left\|\mathrm{vec}\left(\hat{R}(Z)-R\right)\right\|^2_{Q_{\hat{R}(Z)\hat{R}(Z)}} \quad (15)$$

The cost function $C(Z)$ is the sum of two coupled terms: the first weighs the distance from the float ambiguity matrix $\hat{Z}$ to the nearest integer matrix Z in the metric of $Q_{\hat{Z}\hat{Z}}$, while the second weighs the distance from the conditional float solution $\hat{R}(Z)$ to the nearest orthonormal matrix R in the metric of $Q_{\hat{R}(Z)\hat{R}(Z)}$. This rigorous application of the orthonormal constraint results in a non-ellipsoidal search space and requires the computation of a nonlinear constrained least-squares problem (15) for every integer matrix in the search space. In the MC-LAMBDA method, this problem is mitigated through the use of easy-to-evaluate bounding functions (Giorgi and Teunissen 2010). The bounding functions are given as

$$C_{L,T}(Z) = \left\|\mathrm{vec}\left(\hat{Z}-Z\right)\right\|^2_{Q_{\hat{Z}\hat{Z}}} + \lambda_{\min}\sum_{i=1}^{q}(\|\hat{r}_i(Z)\|-1)^2 \quad (16)$$

$$C_{U,T}(Z) = \left\|\mathrm{vec}\left(\hat{Z}-Z\right)\right\|^2_{Q_{\hat{Z}\hat{Z}}} + \lambda_{\max}\sum_{i=1}^{q}(\|\hat{r}_i(Z)\|+1)^2 \quad (17)$$

Using these bounding functions, two strategies, namely the *Expansion* and the *Search and Shrink* strategies, were developed (see e.g. Park and Teunissen 2003; Giorgi et al. 2008). These techniques avoid the computation of (15) for every integer matrix in the search space, and compute the integer minimizer $\check{Z}$ efficiently. In this contribution, we demonstrate that the above bounding functions are relatively loose bounds and may result in too large integer search times in particular for the search and shrink technique. To mitigate this problem, we develop alternative bounding functions in Sect. 3 and evaluate their impacts on performance of the MC-LAMBDA method using simulated as well as real data.

Fixed solution: To obtain the final attitude solution, $\check{Z}$ is substituted into (11), thus giving $\hat{R}(\check{Z})$. This solution has a much better accuracy than $\hat{R}$ (cf. 12), but it is, in general, still non-orthogonal. The sought-for orthogonal attitude solution is then finally obtained by solving (15) for $Z=\check{Z}$.

3 New Bounding Functions

In this section we develop various bounding functions for the following function

$$\min_{R\in\mathbb{O}^{3\times q}}\left\|\mathrm{vec}\left(\hat{R}-R\right)\right\|^2_{Q_{\hat{R}\hat{R}}} \quad (18)$$

with $\mathbb{O}^{3\times q}$ the class of orthogonal matrices, where $q\leq 3$, $\hat{R}$, $Q_{\hat{R}\hat{R}}$ be known real matrices of compatible dimensions. Furthermore, when $q=3$, a proper rotation matrix should satisfy an additional constraint that is the determinant of R is equal to one. In the following sections, we construct

various bounds based on two strategies. The first one is to use a relaxed problem to define bounds for the original problem (Sect. 3.1). The second one is to use a feasible point defining an upper bound (Sect. 3.2). Note that, for notational simplicity, we ignore the dependence of $\hat{R}$ on Z.

3.1 Bounds Based on Relaxation

Elementwise weighting of constrained least-squares problem in (18) does not admit any closed-form solution. However, we can use simplified problems to bound the original problem. If we denote the largest and smallest eigenvalues of $Q^{-1}_{\hat{R}\hat{R}}$ by $\lambda_{\max}$ and $\lambda_{\min}$, respectively, then the function in (18) is bounded as

$$\begin{aligned}
&\min_{R\in\mathbb{O}^{3\times q}} \left\|\operatorname{vec}\left(\hat{R}-R\right)\right\|^2_{\frac{1}{\lambda_{\min}}I} \\
&\leq \min_{R\in\mathbb{O}^{3\times q}} \left\|\operatorname{vec}\left(\hat{R}-R\right)\right\|^2_{Q_{\hat{R}\hat{R}}} \\
&\leq \min_{R\in\mathbb{O}^{3\times q}} \left\|\operatorname{vec}\left(\hat{R}-R\right)\right\|^2_{\frac{1}{\lambda_{\max}}I}
\end{aligned} \tag{19}$$

Note that the minimizers of the above three terms are not necessarily the same. We can, therefore, define bounding functions by solving the following simplified problem

$$\min_{R\in\mathbb{O}^{3\times q}} \left\|\operatorname{vec}\left(\hat{R}-R\right)\right\|^2_{\frac{1}{\lambda}I} \tag{20}$$

Substitution for λ with $\lambda_{\min}$ and $\lambda_{\max}$ will define a lower and an upper bound, respectively, as in (19). In Sect. 3.1.1, we show that the above problem for $q = 3$ is equivalent to the well-known Wahba's problem and use it to define bounding functions.

3.1.1 Wahba Bounds

In Wahba's problem for spacecraft attitude determination (Wahba 1965), the goal is to find an orthogonal matrix with determinant $+1$ that minimizes the following loss function

$$W(R) = \sum_{i=1}^{n} \|x_i - Rs_i\|^2_I \tag{21}$$

where x_i is a set of unit vectors measured in a platform's body frame, s_i are the corresponding unit vectors in a reference frame. The matrix form of the above problem is given as

$$\min_{R\in\mathbb{O}^{3\times 3},\det R=1} \operatorname{tr}\left((X-RS)^T(X-RS)\right) \tag{22}$$

where $S = [s_1,\ldots,s_n]$ and $X = [x_1,\ldots,x_q]$ are the known full column rank matrices, and $\operatorname{tr}(K)$ denotes trace of square matrix K. Using the singular value decomposition, the minimizer of (22) is given as (Markley 1988)

$$\check{R}_W = VDU^T \tag{23}$$

with $D = \operatorname{diag}\left([1,\ 1,\ \det(U)\det(V)]^T\right)$, where U and V are the orthonormal matrices given by the singular value decomposition of SX^T (i.e., $SX^T = U\Sigma V^T$), and $\operatorname{diag}(x)$ refers to the diagonal matrix, whose diagonal elements are defined by elements of vector x. It is easy to see that this problem is a generalization of the problem defined in (20) by substituting with $X = \hat{R}$ and $S = I$, and by scaling with a factor of λ. Using (19) and (23), Wahba bounds are defined as

$$\begin{aligned}
\lambda_{\min}\left\|\operatorname{vec}\left(\hat{R}-\check{R}_W\right)\right\|^2_I &\leq \min_{R\in\mathbb{O}^{3\times q}} \left\|\operatorname{vec}\left(\hat{R}-R\right)\right\|^2_{Q_{\hat{R}\hat{R}}} \\
&\leq \lambda_{\max}\left\|\operatorname{vec}\left(\hat{R}-\check{R}_W\right)\right\|^2_I
\end{aligned} \tag{24}$$

3.2 Bounds Based on Feasible Points

In this section we develop two more upper bounds based on the fact that a feasible point will define an upper bound.

3.2.1 Weighted Wahba Bound

Since the minimizer of Wahba's problem in Sect. 3.1.1 is a feasible point of the original problem in (18), an upper bound is defined as

$$\min_{R\in\mathbb{O}^{3\times q}} \left\|\operatorname{vec}\left(\hat{R}-R\right)\right\|^2_{Q_{\hat{R}\hat{R}}} \leq \left\|\operatorname{vec}\left(\hat{R}-\check{R}_W\right)\right\|^2_{Q_{\hat{R}\hat{R}}} \tag{25}$$

3.2.2 Gram–Schmidt Bound

In this section, we use Gram–Schmidt orthogonalization to obtain a feasible point to the minimization in (18). That is, columns of the feasible point $\check{R}_{GS} = [\check{r}_{1,GS},\ldots,\check{r}_{q,GS}]$ can be written as

$$\check{r}_{i,GS} = \frac{\check{r}'_{i,GS}}{\|\check{r}'_{i,GS}\|_{I_3}}, \text{ with } \check{r}'_{i,GS} = \hat{r}_i - \sum_{j=1}^{i-1} \check{r}^T_{j,GS}\hat{r}_i\check{r}_{j,GS} \tag{26}$$

Using $\check{R}_{GS}$, an upper bound is defined as

$$\min_{R\in\mathbb{O}^{3\times q}} \left\|\operatorname{vec}\left(\hat{R}-R\right)\right\|_{Q_{\hat{R}\hat{R}}} \leq \left\|\operatorname{vec}\left(\hat{R}-\check{R}_{GS}\right)\right\|_{Q_{\hat{R}\hat{R}}} \tag{27}$$

4 Results

In this section we evaluate the effectiveness of various bounding functions using simulated and real data. Due to page limitation, we only show the impact of the upper bounds on MC-LAMBDA's efficiency. We consider three criteria to evaluate the bounds. The first measure is to determine the tightness of the bounds measured by average relative gap (ARG). For an upper bound C_U, ARG is defined as

$$ARG_{C_U} = \frac{1}{N}\sum_{i=1}^{N}\frac{C_U(Z_i) - C(Z_i)}{C(Z_i)} \tag{28}$$

where $C(Z_i)$ is the value of objective function (14) evaluated at Z_i an neighboring integer grid of the optimal integer ambiguity matrix and N is the number of samples. It is easy to see that the bound with the smallest ARG value is the tightest.

The second measure is to determine the complexity of the bounds. We measure numerical computational load by computing average execution time ratio (ATR), which is defined as

$$ATR_{C_x} = \frac{1}{N}\sum_{i=1}^{N}\frac{T_{C_x(Z_i)}}{T_{C(Z_i)}} \tag{29}$$

where $T_{F(\cdot)}$ is the execution time required to compute function $F(\cdot)$. An computationally efficient bound will have small ATR value.

We also measure the effects of bounding functions on the overall computational efficiency of the MC-LAMBDA algorithm. Results from simulation and experimental studies are discussed in Sects. 4.1 and 4.2, respectively.

4.1 Simulation Results

In order to investigate the performance of various bounding functions, we first tested them with simulated data. Table 1 reports simulation set up considered in this work. Based on the location of the receivers and the actual GPS constellation, the design matrices of model (1) were built. A set of 10^5 data was randomly generated with given noise levels (Table 1) for each antenna configuration given in (30). We considered the following antenna configurations: B_0^1 ($q = 1$) a single baseline, B_0^2 ($q = 2$) a planar array with two short baselines (equal length), B_0^3 ($q = 2$) a planar array containing a long baseline and a short baseline, B_0^4 ($q = 3$) a 3D array with three short baselines (equal length), B_0^5 ($q = 3$) a 3D array containing a long baseline and two short baselines, and B_0^6 ($q = 3$) a 3D array (almost planar) to analyze the impact of antenna geometry on MC-LAMBDA computational efficiency.

Table 1 Simulation set up

Date and time	30 July 2010 05:24
Location	Lat: 32° S, Long: 115° E
GPS week	1594
Frequency	L1
Number of satellites (PDOP)	8 (2.71)
Undifferenced code noise	$\sigma_p = 30$ cm
Undifferenced phase noise	$\sigma_\phi = 3$ mm

$$B_0^1 = \begin{bmatrix}2\end{bmatrix},\quad B_0^3 = \begin{bmatrix}20 & 0\\ 0 & 2\end{bmatrix},\quad B_0^5 = \begin{bmatrix}20 & 0 & 0\\ 0 & 2 & 0\\ 0 & 0 & 2\end{bmatrix},$$
$$B_0^2 = \begin{bmatrix}2 & 0\\ 0 & 2\end{bmatrix},\ B_0^4 = \begin{bmatrix}2 & 0 & 0\\ 0 & 2 & 0\\ 0 & 0 & 2\end{bmatrix},\ B_0^6 = \begin{bmatrix}20 & 10 & -10\\ 0 & 10 & 9\\ 0 & 0 & 1\end{bmatrix} \tag{30}$$

Table 2 compares the computational complexities (measured by ATR) of the upper bounds. Note that, one should compare ATR values along the rows, since the objective functions for different dimensions (along columns) are different. From Table 2, it is clear that the evaluation of the bounding functions is at least 20 times faster than that of the original MC-LAMBDA objective function. Even though it shows that the previous bound is the most efficient upper bound, we show in the following that its effectiveness is relatively poor due to looseness.

The tightness (measured by ARG) of the upper bounding functions are compared in Table 3 summarizing the impact of antenna geometry on ARG value. One should compare ARG values along the rows, since the objective functions for different dimensions (along columns) are different. These results clearly indicate that the previous bound is indeed loose. Except for a few cases, the Gram–Schmidt based bound is the tightest bound. Furthermore, one can make the Gram–Schmidt based bound tighter by choosing the order of baselines. That is, one should choose long baselines first and then short baselines. Reversing the order results in a looser bound (given between brackets in Table 3). All other upper bounds are invariant to baseline permutations and looser than the Gram–Schmidt based bound, as they do not utilize the structure of $Q_{\hat{R}(Z)\hat{R}(Z)}$.

Finally, we compared the impacts of upper bounding functions on MC-LAMBDA efficiency. The average overall computation times for MC-LAMBDA processing using different bounds are summarized in Table 4. It clearly shows that a tighter bound (Table 3) results in a shorter search time. The Gram–Schmidt based bound is most effective compared with all other bounds.

Table 2 Computational complexity of upper bounds: average time ratio; the least computational complexity bounds are highlighted using bold text

	Previous bound C_{2T} from (17)	Wahba bound C_{2W} based on (24)	Weighted Wahba bound C_{2WW} based on (25)	Gram–Schmidt bound C_{2GS} based on (27)
$q = 1$	**0.006**	0.011	0.022	0.016
$q = 2$	**0.005**	0.029	0.035	0.025
$q = 3$	**0.005**	0.035	0.041	0.038

Table 3 Tightness of upper bounds: average relative gap vs. the antenna configuration; the tightest bounds are highlighted using bold text

	Previous bound C_{2T} from (17)	Wahba bound C_{2W} based on (24)	Weighted Wahba bound C_{2WW} based on (25)	Gram–Schmidt bound C_{2GS} based on (27)
B_0^1	4090	1.01	**0.21**	**0.21**
B_0^2	3740	2.2	**0.32**	0.45
B_0^3	290000	59.9	12.7	**0.31** (13)
B_0^4	2240	3.93	**0.17**	1.38
B_0^5	245000	173	18.6	**0.77** (79)
B_0^6	372000	1310	166	**0.75**

The terms between brackets correspond to the reverse order of baselines (short baselines first and then long baselines)

Table 4 Average computation time (s) vs the antenna configuration ("*" refers to times longer than 1 s); the most efficient bounds are highlighted using bold text

	Previous bound C_{2T} from (17)	Wahba bound C_{2W} based on (24)	Weighted Wahba bound C_{2WW} based on (25)	Gram–Schmidt bound C_{2GS} based on (27)
B_0^2	*	0.060	**0.013**	**0.013**
B_0^3	*	*	0.156	**0.020**
B_0^4	*	0.207	**0.020**	0.029
B_0^5	*	*	0.277	**0.038**
B_0^6	*	*	*	**0.034**

4.2 Experimental Results

In the experiment analyses, we consider an aerial remote sensing campaign held on 1 November 2007 in the Netherlands with several GPS antennas/receivers mounted on the Cessna Citation II aircraft of the Faculty of Aerospace Engineering, Delft University of Technology, The Netherlands. The aircraft equipped with three GNSS antennas: one on the body, approximately in the middle of the fuselage (S67-1575-96 type L1/L2 sensor system), one on the wing, and one on the nose (both L1 sensor system) forming the following antenna geometry (Fig. 1),

$$B_0 = \begin{bmatrix} 4.90 & -0.39 \\ 0 & 7.60 \end{bmatrix} \quad \text{(m)} \tag{31}$$

All three antennas were connected to a Septentrio PolaRx2@ receiver, logging data for the entire duration of the flight, from 10:06 to 14:18 (UTC time).

We considered the most challenging scenario, namely single-epoch, single frequency, unaided ambiguity resolution, and compared the performance of the MC-LAMBDA method with that of the standard LAMBDA method. MC-LAMBDA processing yields a high integer resolution success rate (96.4 %), while standard LAMBDA processing yields a low success rate (28.1 %). This improved performance is due to the multivariate orthonormality constraint, which however requires more computational effort. The average computation times for MC-LAMBDA (with new tighter Gram–Schmidt bound) and standard LAMBDA are 0.81 and 0.01 s, respectively. Finally, we compared MC-LAMBDA (GPS) estimates for attitude angles with output of an Inertial Navigation System (INS), the Honeywell Laseref II IRS (YG1782B), on board. The standard deviations of the GPS-INS angular differences are 0.06° for heading, 0.15° for elevation, and 0.10° for bank. The heading angle is estimated with the highest precision, whereas the elevation shows the highest noise level.

5 Conclusions

The Multivariate Constrained (MC-)LAMBDA method exploits the a priori knowledge of the complete antenna geometry. This strengthens the observation model and hence improves the capacity of fixing the correct set of integer ambiguities. This rigorous inclusion of the geometrical constraints enables instantaneous attitude determination

using GNSS. In this contribution we developed various easy-to-compute bounding functions for the ambiguity objective function of the MC-LAMBDA method. First we described the GNSS attitude model and the principles of the MC-LAMBDA method. Then we proposed various upper and lower bounds for the MC-LAMBDA objective function. We demonstrated the effectiveness of the new bounding functions using simulated and real data. Gram–Schmidt based bound, in general, is most effective improving the overall performance of MC-LAMBDA method. Finally, the superior success rate performance of the MC-LAMBDA method compared to the unconstrained LAMBDA method in a high dynamic environment was demonstrated. We considered the most challenging application being single-frequency, single epoch GPS-only ambiguity resolution and attitude determination. However, one can consider multi-frequency, multi epoch multi-GNSS observations that strengthen the underlying model and hence improve the performance of ambiguity resolution and attitude determination.

References

Cohen C (1992) Attitude determination using GPS. Ph.D. Thesis, Stanford University

Crassidis JL, Markley FL (1997) New algorithm for attitude determination using Global Positioning System signals. J Guid Contr Dynam 20(5):891–896

Giorgi G, Teunissen PJG (2010) Carrier phase GNSS attitude determination with the multivariate constrained LAMBDA method. In: Aerospace conference, 2010. IEEE, New York, pp 1–12

Giorgi G, Teunissen PJG, Buist PJ (2008) A search and shrink approach for the baseline constrained LAMBDA method: experimental results. In: Yasuda A (ed) Proceedings of international symposium on GPS/GNSS. Tokyo University of Marine Science and Technology, Tokyo, pp 797–806

Li Y, Zhang K, Roberts C, Murata M (2004) On-the-fly GPS-based attitude determination using single- and double-differenced carrier phase measurements. GPS Solut 8(2):93–102

Lin D, Voon L, Nagarajan N (2004) Real-time attitude determination for microsatellite by LAMBDA method combined with Kalman filtering. In: 22nd AIAA international communications satellite systems conference and exhibit 2004, Monterey, CA, USA

Lu G (1995) Development of a GPS multi-antenna system for attitude determination. Ph.D. Thesis, Engineering Department of Geomatics Engineering, University of Calgary

Madsen J, Lightsey EG (2004) Robust spacecraft attitude determination using global positioning system receivers. J Spacecr Rockets 41(4):635–643

Markley FL (1988) Attitude determination using vector observations and the singular value decomposition. J Astronaut Sci 36(3): 245–258

Park C, Teunissen PJG (2003) A new carrier phase ambiguity estimation for GNSS attitude determination systems. In: Proceedings of international symposium on GPS/GNSS, Tokyo, Japan

Psiaki ML (2006) Batch algorithm for global-positioning-system attitude determination and integer ambiguity resolution. J Guid Contr Dynam 29(5):1070–1079

Teunissen PJG (2007) A general multivariate formulation of the multi-antenna GNSS attitude determination problem. Artif Satell 42(2):97–111

Wahba G (1965) Problem 65-1: a least squares estimate of spacecraft attitude. SIAM Rev 7(3):409